

## First Light Curve Analysis of NSVS 8294044, V1023 Her, and V1397 Her Contact Binary Systems

ATILA PORO,<sup>1,\*</sup> SABRINA BAUDART,<sup>2</sup> MAHSHID NOURMOHAMMAD,<sup>3</sup> ZAHRA SABAGHPOUR ARANI,<sup>4</sup> FATEMEH FARHADI,<sup>5</sup> SELDA RANJBAR SALEHIAN,<sup>6</sup> AHMAD SAROSTAD,<sup>7</sup> SAEIDEH RANJBARYAN IRI OLYA,<sup>8</sup> MARYAM HADIZADEH,<sup>9</sup> AND AMIRHOSSEIN KHODAEI<sup>5</sup>

<sup>1</sup> Astronomy Department of the Raderon AI Lab., BC., Burnaby, Canada

<sup>2</sup> Double Stars Committee, Société Astronomique de France, Paris, France

<sup>3</sup> Independent Astrophysics Researcher, Isfahan, Iran

<sup>4</sup> Akhtaran Astronomical Society, Isfahan Province, Aran and Bidgol, Iran

<sup>5</sup> Department of Physics, Faculty of Science, Zanjan University, Zanjan, Iran

<sup>6</sup> Astronomy Students' Scientific Association, University of Tabriz, East Azerbaijan Province, Tabriz, Iran

<sup>7</sup> Yazd Desert Night Sky Astronomy Institute, Yazd Province, Yazd, Iran

<sup>8</sup> Ayaz Astronomical Association, East Azerbaijan Province, Tabriz, Iran

<sup>9</sup> Khayyam Astronomy Association, Fars, Fasa, Iran

### ABSTRACT

The first photometric light curve investigation of the NSVS 8294044, V1023 Her, and V1397 Her binary systems is presented. We used ground-based observations for the NSVS 8294044 system and Transiting Exoplanet Survey Satellite (TESS) data for V1023 Her and V1397 Her. The primary and secondary times of minima were extracted from all the data, and by collecting the literature, a new ephemeris was computed for each system. Linear fits for the O-C diagrams were conducted using the Markov chain Monte Carlo (MCMC) method. Light curve solutions were performed using the PHysics Of Eclipsing BinariEs (PHOEBE) Python code and the MCMC approach. The systems were found to be contact binary stars based on the fillout factor and mass ratio. V1023 Her showed the O'Connell effect, and a cold starspot on the secondary component was required for the light curve solution. The absolute parameters of the system were estimated based on an empirical relationship between orbital period and mass. We presented a new  $T - M$  equation based on a sample of 428 contact binary systems and found that our three target systems were in good agreement with the fit. The positions of the systems were also depicted on the  $M - L$ ,  $M - R$ ,  $q - L_{ratio}$ , and  $M_{tot} - J_0$  diagrams in the logarithmic scales.

**Keywords:** binaries: eclipsing – methods: photometry – stars: individual (NSVS 8294044)

### 1. INTRODUCTION

The degree of separation between the components describes different kinds of eclipsing binaries, which may be identified by light curve shapes and include detached, semi-detached, contact, and overcontact systems. Contact binary stars are referred to as W UMa-type systems that have some interesting physical properties (Drake et al. 2014).

Stars of the W UMa systems have filled their Roche lobes (Paczynski 1971) and both of the components share a common convective envelope between the inner and outer contact surfaces (Lucy 1968). The stars in these kinds of systems share mass and energy, which causes their surface temperatures to be close to one another and show light curves with almost similar eclipse depths. Furthermore, W UMa stars consist of late spectral type main sequence stars (Terrell et al. 2012).

The orbital period of contact binary systems is short and most of them fall between 0.2 and 0.6 days (Qian 2003, Kouzuma 2018, Latković et al. 2021). Studying contact systems provides an opportunity to use orbital period variations impacted by system physical processes to gain a deeper comprehension of star evolution (Li et al. 2021). Therefore, new observations can always be useful to investigate these variations.

\* poroatila@gmail.com

This study includes the first light curve analysis of three binary systems NSVS 8294044 (R.A.  $19^h 14^m 41.0475^s$ , Dec.  $+37^\circ 49' 46.0465''$  (J2000)), V1023 Her (R.A.  $15^h 58^m 25.2669^s$ , Dec.  $+49^\circ 26' 51.0013''$  (J2000)), and V1397 Her (R.A.  $17^h 07^m 16.8455^s$ , Dec.  $+17^\circ 25' 36.6323''$  (J2000)). All three target systems have been introduced as contact systems in the ASAS<sup>1</sup> and VSX<sup>2</sup> catalogs. NSVS 8294044, V1023 Her, and V1397 Her's orbital periods are near to each other as reported at 0.3779846, 0.3222336, and 0.387745 days in the VSX database, respectively. Also, the apparent magnitude of the NSVS 8294044 is  $V_{max} = 13.51^{mag}$ , V1023 Her is  $V_{max} = 11.93^{mag}$ , and V1397 Her is  $V_{max} = 10.16^{mag}$ , based on the VSX database.

The structure of this paper is as follows: Section 2 is about ground- and space-based observations and data reduction; Section 3 is related to determining new ephemeris for each system; Section 4 explains the light curve analysis; Section 5 describes the estimation of absolute parameters; Finally, the discussion and conclusion are in Section 6.

## 2. OBSERVATION AND DATA REDUCTION

We observed NSVS 8294044 in August and September 2023. The observations were carried out in a private observatory in Toulon, France, at a longitude of  $05^\circ 54' 35''$  E and a latitude of  $43^\circ 8' 59''$  N, and an altitude of 68 meters above mean sea level. In the observations, we used an Apochromatic Refractor TS Optics with a 102mm aperture, a ZWO ASI 1600MM CCD, and a  $V$  filter. The binning of the images was  $1 \times 1$ , with an 80-second exposure time, and the average temperature of the CCD was  $-15^\circ\text{C}$ . Using the Siril 1.2.0-rc2 program and the bias, dark, and flat fields image, the basic data reduction was done. We used GSC 02665-00244 (R.A.  $19^h 17^m 21.4390^s$ , Dec.  $+37^\circ 11' 51.0482''$  (J2000)) as a comparison star, and GSC 02665-01066 (R.A.  $19^h 17^m 11.7567^s$ , Dec.  $+37^\circ 13' 32.9641''$  (J2000)) and Gaia DR2 2051151521582207232 (R.A.  $19^h 17^m 06.8187^s$ , Dec.  $+37^\circ 04' 22.3909''$  (J2000)) as check stars. According to our observations, the light curve's maximum apparent magnitude was obtained to be  $V_{max} = 13.24(11)^{mag}$ .

TESS data were used in this investigation for V1023 Her (TIC 310170498) and V1397 Her (TIC 143100813) binary systems. TESS observed V1023 Her in sectors 23, 24, 50, and 51. There were also observational data for the V1397 Her system in sectors 12 and 13. TESS employed a 120-second exposure time for the observation process of these sectors. The data is available at the Mikulski Space Telescope Archive (MAST)<sup>3</sup>.

## 3. NEW EPHEMERIS

We extracted the primary and secondary times of minima from ground-based and TESS light curves. Gaussian distribution was used to determine these mid-eclipse times. The amount of uncertainty was computed using the MCMC method. The Barycentric Julian Date and Barycentric Dynamic Time ( $BJD_{TDB}$ ) are used to present all minima. The minima for three target systems that were collected from the literature and extracted in this study are listed in Table 1. The extracted TESS mid-eclipse times for the V1023 Her and V1397 Her systems are listed in the appendix tables.

Each epoch and O-C values were computed using reference ephemeris. We chose  $t_0 = 2458423.7230$  and  $P_{ref} = 0.3779833$  from the ASAS-SN catalog for the NSVS 8294044 system as a reference ephemeris. V1023 Her's  $t_0 = 2459636.8875$  came from Nelson & Alton (2022) study and  $P_{ref} = 0.3222341(87)$  from the WISE catalog of periodic variable stars. The reference ephemeris of V1397 Her  $t_0 = 2453833.6397$  and  $P_{ref} = 0.387745$  were from the Diethelm (2009) study.

<sup>1</sup> The All Sky Automated Survey (ASAS), <http://www.astrowww.edu.pl/asas/>

<sup>2</sup> The International Variable Star Index (VSX), <https://www.aavso.org/vsx/>

<sup>3</sup> <https://mast.stsci.edu/portal/Mashup/Clients/Mast/Portal.htmlL>

**Table 1.** The times of minima extracted in this study and collected from the literature were observed with CCD.

System	Min.( $BJD_{TDB}$ )	Error	Epoch	O-C	Reference
NSVS 8294044	2458423.7230		0	0	ASAS-SN
	2460176.4440	0.0012	4637	0.0124569	This study
	2460191.3750	0.0022	4676.5	0.01314655	This study
V1023 Her	2451274.6148		-25951	0.0244	ROTSE- Anton Paschke
	2455976.6448		-11359	0.0144	VSX
	2456687.9726	0.0002	-9151.5	0.0105	Nelson (2015)
	2456745.4889	0.0024	-8973	0.0080	Hubscher & Lehmann (2015)
	2457100.4327	0.0029	-7871.5	0.0109	Hubscher (2016)
	2457100.5900	0.0019	-7871	0.0071	Hubscher (2016)
	2457122.8228	0.0020	-7802	0.0057	Nelson (2016)
	2459636.8875		0	0	Nelson & Alton (2022)
V1397 Her	2453833.6397		0	0	Diethelm (2009)
	2454623.6747		2037.5	0.0046	VSX
	2454998.8205	0.0007	3005	0.0070	Diethelm (2009)
	2455720.8049	0.0003	4867	0.0102	Diethelm (2011)
	2456054.8507	0.0005	5728.5	0.0137	Diethelm (2012)
	2458626.0127		12359.5	0.0386	Kazuo (2020)
	2458991.4659	0.0008	13302	0.0422	Pagel (2021)
	2459383.4822	0.0013	14313	0.0483	Pagel (2022)

It is more appropriate to use a linear fit for O-C diagrams considering our three binary systems have few observations and minimum times. O-C diagrams of the systems are presented in Figure 1 with their corner plots of the posterior distribution based on the MCMC sampling. To determine new ephemeris for each system, we applied 20 walkers and 20000 iterations for each walker, with a 2000 burn-in period in the MCMC process. So, we used the PyMC3 package to execute the MCMC sampling (Salvatier et al. 2016). New ephemeris for each target system is presented in Equations 1 to 3:

$$\begin{cases} \text{NSVS 8294044 :} \\ \text{Min.}I(BJD_{TDB}) = 2458423.72300(10) + 0.377986034(9) \times E \end{cases} \quad (1)$$

$$\begin{cases} \text{V1023 Her :} \\ \text{Min.}I(BJD_{TDB}) = 2459636.89178(1) + 0.322233134(3) \times E \end{cases} \quad (2)$$

$$\begin{cases} \text{V1397 Her :} \\ \text{Min.}I(BJD_{TDB}) = 2453833.63457(8) + 0.387748745(6) \times E \end{cases} \quad (3)$$

#### 4. LIGHT CURVE ANALYSIS

We utilized the PHOEBE Python code version 2.4.9 and the MCMC approach to model the light curves of the NSVS 8294044, V1023 Her, and V1397 Her binary systems (Prša & Zwitter 2005, Prša et al. 2016, Conroy et al. 2020). These three target systems were analyzed for the first time. We selected contact mode for the light curve solutions based on the appearance of the light curve and short orbital period. The gravity-darkening coefficients and the bolometric albedo were assumed to be  $g_1 = g_2 = 0.32$  (Lucy 1967) and  $A_1 = A_2 = 0.5$  (Ruciński 1969), respectively. The limb darkening coefficients were included in PHOEBE as a free parameter, and the Castelli & Kurucz (2004) study was used to model the stellar atmosphere.

We applied the effective temperature reported from Gaia DR3 to the hotter star. These temperature values are not fixed and will be free parameters during the MCMC process. The effective temperature ratio was used to estimate the

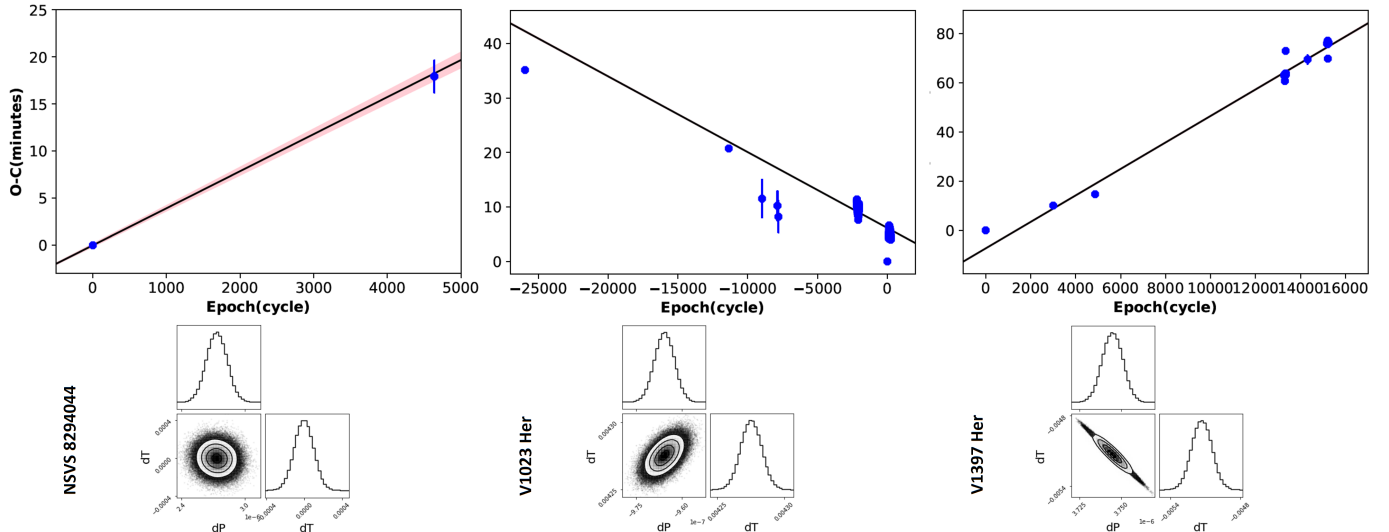


**Figure 1.** The O-C diagrams of three eclipsing binaries with linear fits and corner plots. The shaded regions show the model parameters' 68th percentile values.

initial temperature of another component. Additionally, we checked and compared the effective temperatures of these systems from TESS through the MAST portal<sup>4</sup>. The TESS input v8.2 reported temperatures 5937(115), 5088(126), and 6440(113) for NSVS 8294044, V1023 Her, and V1397 Her, respectively. These values were close to those reported by Gaia DR3.

The  $q$ -search method was used to estimate the mass ratio of each binary system, taking into account that only photometric data was available. We performed a  $q$ -search on each of the target systems using a range of 0.1 to 9. We found the minimum sum of the squared residuals for each  $q$ -search. We used the results as initial values and tried to fit a good synthetic light curve to the observational data. Figure 2 displays the  $q$ -search results for each of the three systems.

V1023 Her system's light curve analysis required a cold starspot on the secondary component due to the difference in the light curve maxima. Contact systems are known for their magnetic activity, and O'Connell's effect describes it (O'Connell 1951).

We employed PHOEBE's optimization tool to improve the output of light curve solutions and obtain entitled results for beginning the MCMC process. The five main parameters ( $T_1$ ,  $T_2$ ,  $q$ ,  $f$ ,  $l_1$ ) were then processed using the MCMC approach, and the values and uncertainty were obtained. We employed 96 walkers and 1000 iterations for each walker. These walkers were initially positioned from a Gaussian distribution based on our initial parameter estimations, and their width was adjusted based on how sensitive the light curves were to various parameter values.

The results of the light curve solutions of the NSVS 8294044, V1023 Her, and V1397 Her binary systems are listed in Table 2. The observed and synthetic light curves of the binary systems, along with the corner plots, are displayed in Figure 3. Furthermore, the geometric structures of the systems are shown in Figure 4.

## 5. ABSOLUTE PARAMETERS

We used empirical parameter relationships between mass and orbital period for estimating absolute parameters (Poro et al. 2024). So, the following equation was chosen from the Latković et al. (2021) study result of a large sample:

$$M_1 = (2.94 \pm 0.21)P + (0.16 \pm 0.08) \quad (4)$$

<sup>4</sup> <https://mast.stsci.edu/portal/Mashup/Clients/Mast/Portal.htmlL>

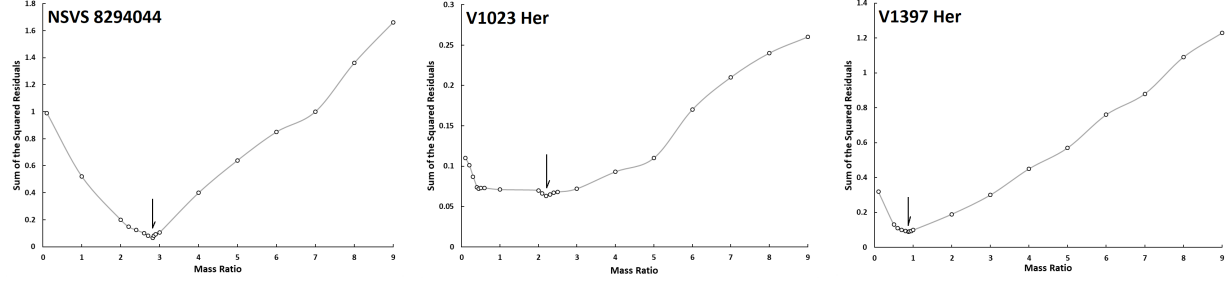


**Figure 2.** Sum of the squared residuals as a function of the mass ratio.

**Table 2.** Photometric light curve solutions of the systems.

Parameter	NSVS 8294044	V1023 Her	V1397 Her
$T_1$ (K)	$6070^{+(320)}_{-(120)}$	$4980^{+(6)}_{-(6)}$	$6326^{+(10)}_{-(6)}$
$T_2$ (K)	$5630^{+(290)}_{-(100)}$	$4624^{+(6)}_{-(7)}$	$6413^{+(13)}_{-(8)}$
$q = M_2/M_1$	$2.819^{+(75)}_{-(69)}$	$2.199^{+(28)}_{-(25)}$	$0.873^{+(23)}_{-(11)}$
$i^\circ$	$83.68^{+(99)}_{-(79)}$	$48.54^{+(32)}_{-(21)}$	$65.98^{+(10)}_{-(15)}$
$f$	$0.152^{+(23)}_{-(25)}$	$0.121^{+(8)}_{-(13)}$	$0.112^{+(9)}_{-(6)}$
$\Omega_1 = \Omega_2$	6.282(41)	5.458(37)	3.486(24)
$l_1/l_{tot}$	$0.359^{+(3)}_{-(3)}$	$0.406^{+(1)}_{-(1)}$	$0.520^{+(1)}_{-(4)}$
$l_2/l_{tot}$	0.641(3)	0.594(1)	0.480(2)
$r_1(mean)$	0.303(2)	0.322(2)	0.402(3)
$r_2(mean)$	0.491(2)	0.459(2)	0.378(3)
Phase shift	0.033(1)	-0.012(1)	0.003(1)
Col.(deg)		107	
Long.(deg)		320	
Rad.(deg)		16	
$T_{spot}/T_{star}$		0.92	
Component		Secondary	

Was considered on  $q' = 1/q$  in the Latković et al. (2021) sample and points mentioned in the Poro et al. (2024) study. Therefore, we set the outcome's mass from Equation 4 for the more massive star in the systems. Using the mass ratio from the light curve solution, we obtained the mass of the other companion star. Then, we computed  $a(R_\odot)$  by employing Kepler's third law. We estimated the radius of the stars of the system from the equation  $R = a \times r(mean)$ . The known equation  $L = 4\pi R^2 \sigma T^4$  is also used to determine each star's luminosity while having its effective temperature and radius. Based on Pogson's relation (Pogson 1856),  $M_{bol1,2}$  can be calculated by  $M_{bol} - M_{bol\odot} = -2.5 \log(L/L_\odot)$ , which  $M_{bol\odot}$  is taken as 4.73 magnitude (Torres 2010). We extracted the Bolometric Correction (BC) from the Flower (1996) study tables and utilized the well-known equation  $M_V = M_{bol} - BC$  to compute  $M_{V1,2}$ . The surface gravity ( $g$ ) of the stars was calculated with the equation  $g = G_\odot(M/R^2)$ .

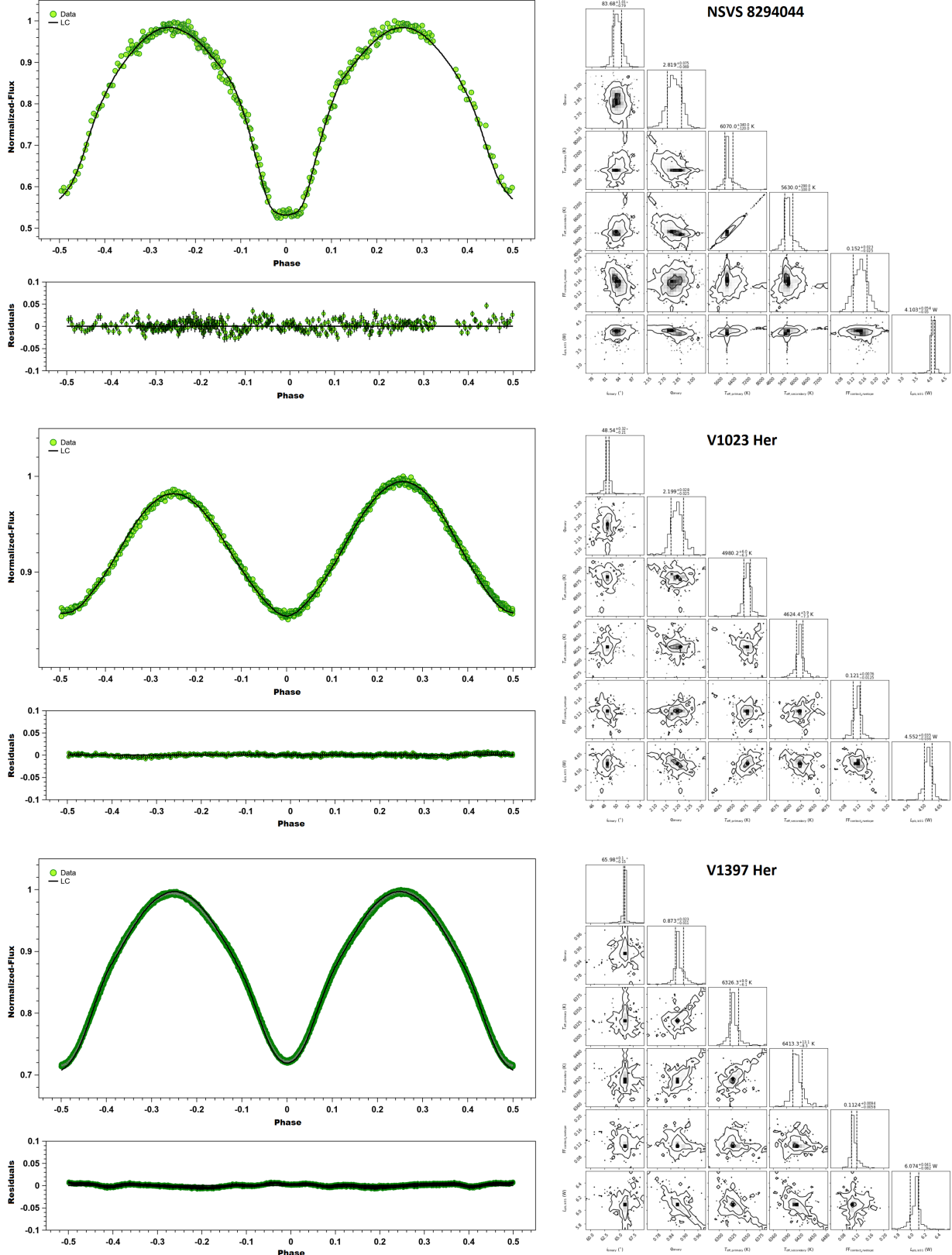


**Figure 3.** Left: The observed light curves of the systems (green dots) and the synthetic light curves were obtained from the light curve solutions (black curves). Right: The corner plots of the three systems were determined by MCMC modeling.

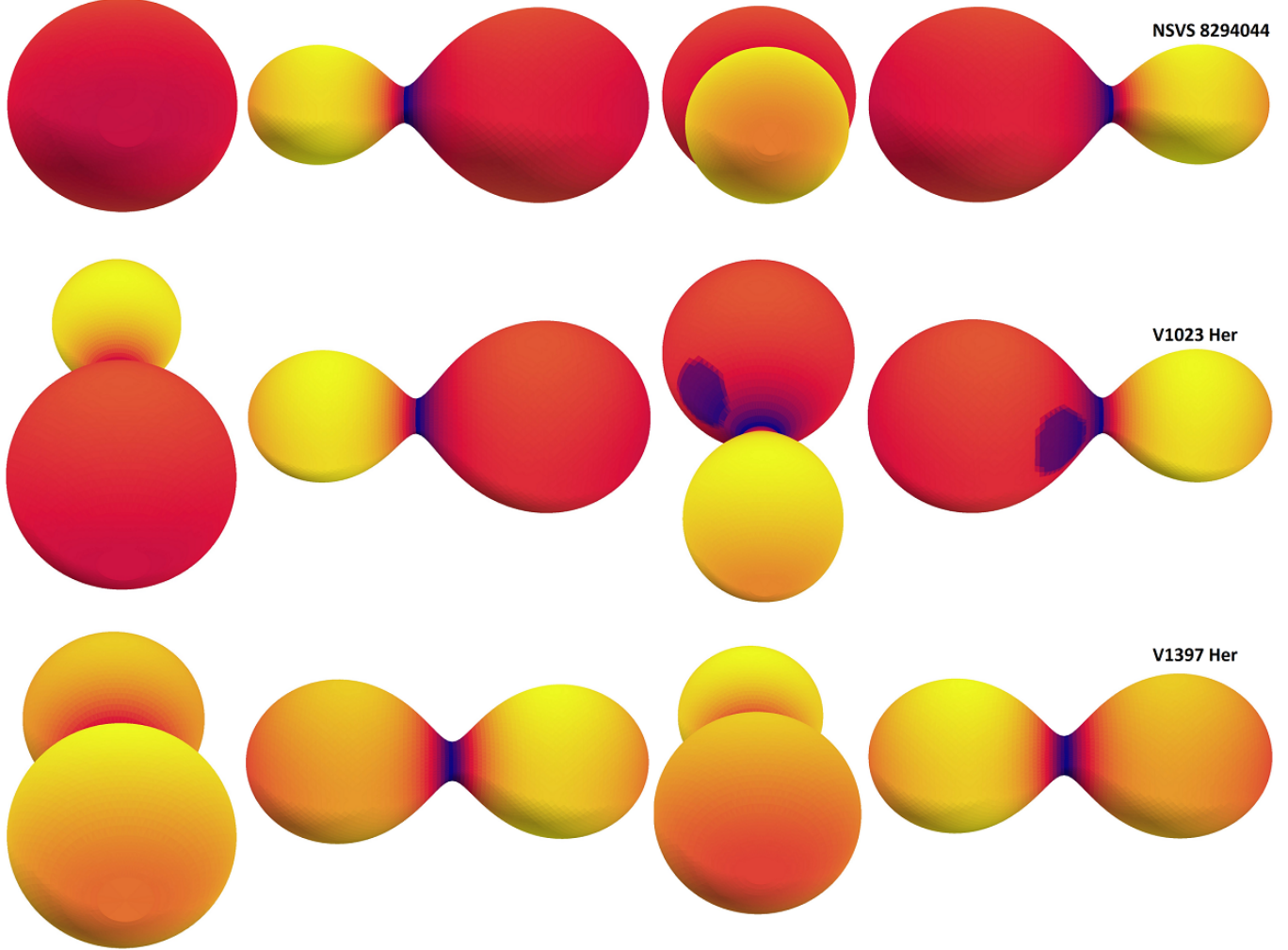


**Figure 4.** Geometric structure of the NSVS 8294044, V1023 Her, and V1397 Her systems based on their light curve solutions in 0, 0.25, 0.5, and 0.75 phases.

**Table 3.** The absolute parameters estimation.

Parameter	NSVS 8294044		V1023 Her		V1397 Her	
	Primary star	Secondary star	Primary star	Secondary star	Primary star	Secondary star
$M(M_{\odot})$	0.451(44)	1.271(160)	0.503(61)	1.107(148)	1.300(161)	1.135(165)
$R(R_{\odot})$	0.799(189)	1.295(303)	0.746(170)	1.064(240)	1.210(216)	1.138(204)
$L(L_{\odot})$	0.781(512)	1.518(962)	0.309(159)	0.467(239)	2.114(836)	1.974(788)
$M_{bol}(\text{mag.})$	4.998(547)	4.277(533)	6.005(451)	5.558(448)	3.917(362)	3.992(365)
$M_V(\text{mag.})$	5.034(547)	4.386(533)	6.320(451)	6.074(448)	3.925(362)	3.993(365)
$\log(g)(\text{cgs})$	4.287(144)	4.318(131)	4.394(129)	4.428(122)	4.386(92)	4.381(84)
$a(R_{\odot})$	2.637(604)		2.318(511)		3.010(511)	
$\log J_0$	51.632(76)		051.606(86)		51.996(91)	
$BC$	-0.036	-0.109	-0.315	-0.516	-0.008	-0.001

Estimated absolute parameters for the target systems are presented in Table 3. The error values of Equation 4 and the parameters involved were used to estimate the absolute parameter uncertainty.

## 6. DISCUSSION AND CONCLUSION

We present the first light curve analysis of the NSVS 8294044, V1023 Her, and V1397 Her binary systems. Ground-based observations were used for NSVS 8294044, and TESS observations were used for V1023 Her and V1397 Her systems. The discussion and conclusion are presented as follows:

1. We extracted times of minima from ground- and space-based photometric data. Thus, by adding the literature, new ephemeris for each system were obtained. A linear fit was the better option for the target systems on the O-C diagram. The O-C diagram of V1023 Her has a decreasing trend based on the linear fit, whereas systems NSVS 8294044 and V1397 Her display an increasing trend (Figure 1).

2. Light curve analysis of each target binary system was performed and V1023 Her required a cold starspot. The results of light curve solutions indicate that the effective temperature range of the stars is between about 4600 K and 6400 K. Star1 is hotter than star2 except for system V1397 Her. The temperature difference of the components for NSVS 8294044 is 440 K, for V1023 Her is 356 K, and for V1397 Her is 87 K. According to the temperature of the stars and the Cox (2000) and Eker et al. (2018) studies, the spectral type of the stars can be recognized: Star1=G0 and star2=G7 for NSVS 8294044; Star1=K1 and star2=K3 for V1023 Her; Star1=F6 and star2=F5 for V1397 Her.

3. We used an empirical parameter relationship and orbital periods for estimating the mass of each star. According to the absolute parameters, we showed the stars' positions on the Mass-Luminosity ( $M - L$ ) and Mass-Radius ( $M - R$ ) diagrams with the Zero-Age Main Sequence (ZAMS) and the Terminal-Age Main Sequence (TAMS) (Figure 5a,b). The position of the systems on the  $q - L_{ratio}$  relationship provided by Poro et al. (2024) are also displayed in Figure 5c, with which they are in good agreement with the model.

4. We calculated the orbital angular momentum ( $J_0$ ) of the systems based on the equation presented by the Eker et al. (2006) study:

$$J_0 = \frac{q}{(1+q)^2} \sqrt[3]{\frac{G^2}{2\pi} M^5 P} \quad (5)$$

The results are listed in Table 3. Furthermore, as can be viewed in Figure 5d, the  $\log M_{tot} - \log J_0$  diagram illustrates the systems' positions and indicates that all of them are located in the region of contact binary systems. The parabolic fit in Figure 5d of the border between the two detached and contact binaries comes from the Eker et al. (2006) study.

5. The relationship between parameters in binary systems is one of the topics of interest in studies. However, most of the investigations on the mass-temperature ( $M - T$ ) relationship have focused on detached and semi-detached binary systems (e.g. Paczyński 1967, Harmanec 1988, Kovaleva 2002, Malkov 2007, Spada et al. 2013, Eker et al. 2018). In the Yakut & Eggleton (2005) study, the  $\log M - \log T$  diagram for contact binaries displays a sample of A- and W-type systems with a ZAMS line. Additionally, the  $M - T$  diagram for a limited number of contact systems in the Kjurkchieva et al. (2019) study indicates a weak relationship for this sample given the large dispersion that appears.

The relationship between  $P - T_1 - M_1$  is presented using a machine learning model in another work by Poro et al. (2024). They employed 134 contact systems that were analyzed using spectroscopic data. This model is presented using the Artificial Neural Network (ANN) and  $M_1$  is the more massive component of the system. Based on the ANN model, more massive stars 1.20(8), 0.99(9), and 1.27(6) have been estimated for systems NSVS 8294044, V1023 Her, and V1397 Her, respectively; these values are in the uncertainty range and good in agreement with the results of this study.

We provided the  $T_1 - M_m$  diagram with a linear fit using 428 contact systems from the sample of the Latković et al. (2021) study (Equation 6). We named the more massive star  $M_m$ . Figure 6 shows the positions of our three target systems are in good agreement with this fit and the other stars in the sample.

$$\log M_m = (1.6185 \pm 0.0150) \times \log T_1 + (-6.0186 \pm 0.0562) \quad (6)$$

6. The first light curve study of binary stars is important to create larger samples for deeper parameter investigations of these types of systems. This investigation presented the new ephemeris and the first light curve analysis of the target binary systems. We concluded that NSVS 8294044, V1023 Her, and V1397 Her are contact binary systems based on the mass ratio, fillout factor, inclination, absolute parameters, and the  $\log M_{tot} - \log J_0$  diagram.

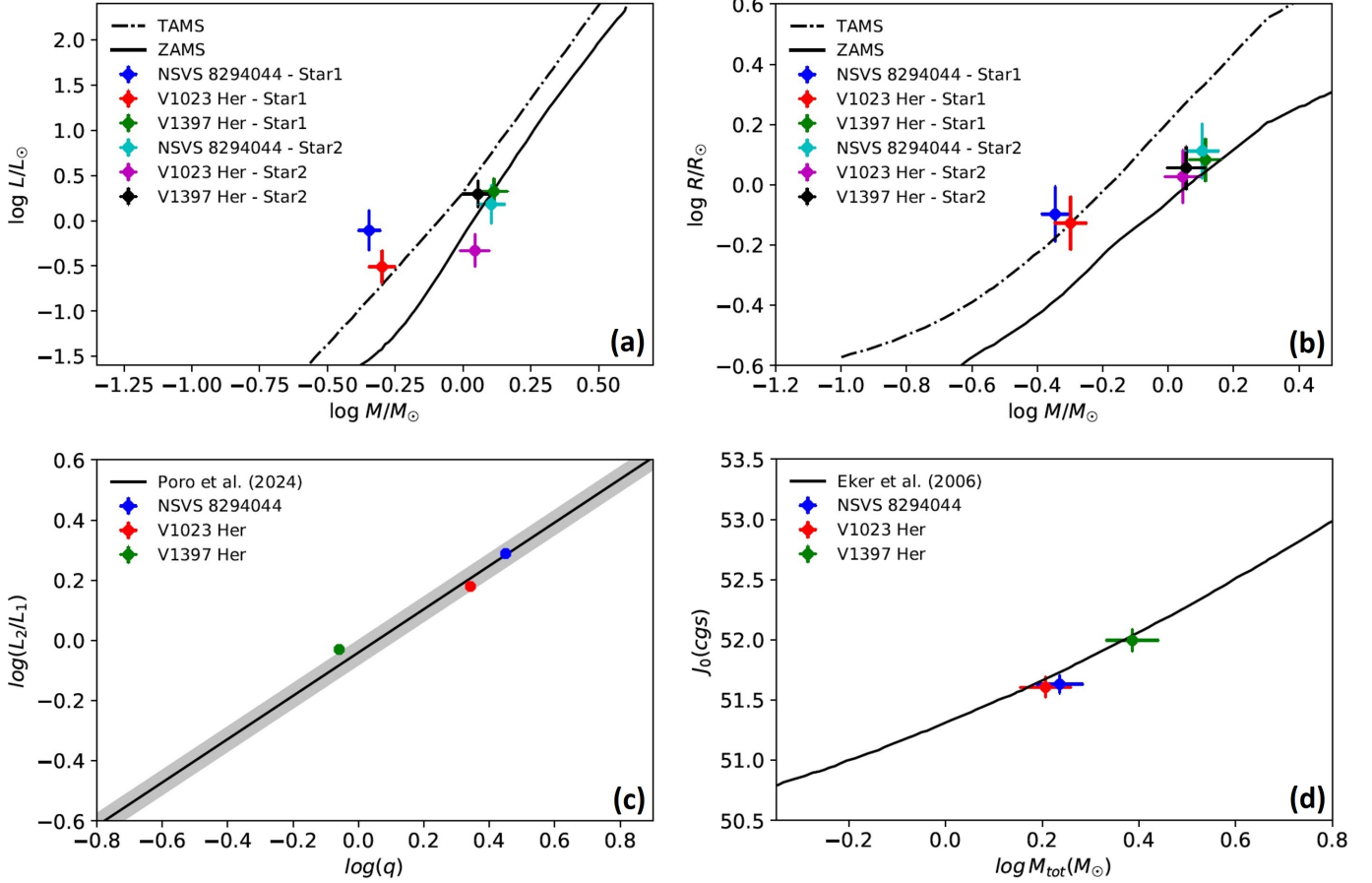


**Figure 5.** The  $\log M - \log L$ ,  $\log M - \log R$ ,  $\log q - \log L_{\text{ratio}}$ , and  $\log M_{\text{tot}} - \log J_0$  diagrams.

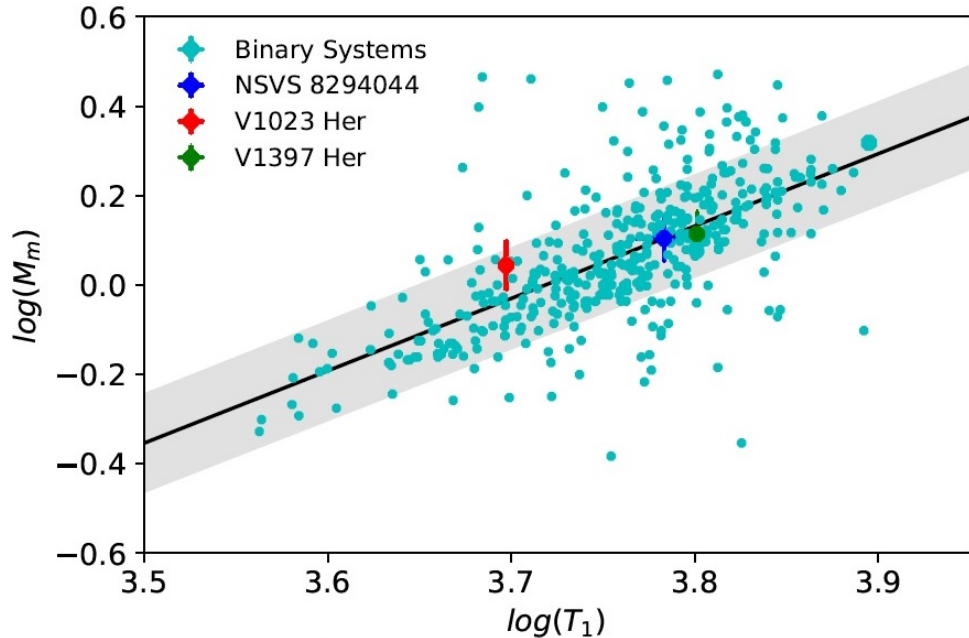


**Figure 6.** Diagram of the effective temperature ( $T_1$ ) and more massive component ( $M_m$ ) of the contact binary systems.

## DATA AVAILABILITY

Ground-based data will be made available on request.

## ACKNOWLEDGEMENTS

This manuscript was prepared by the BSN project (<https://bsnp.info/>). We have made use of data from the European Space Agency (ESA) mission Gaia (<http://www.cosmos.esa.int/gaia>), processed by the Gaia Data Processing and Analysis Consortium (DPAC). This work includes data from the TESS mission observations. Funding for the TESS mission is provided by the NASA Explorer Program.

## ORCID IDS

Atila Poro: 0000-0002-0196-9732  
 Sabrina Baudart: 0009-0004-8426-4114  
 Mahshid Nourmohammad: 0009-0006-0476-2055  
 Zahra Sabaghpour Arani: 0009-0009-7505-9190  
 Fatemeh Farhadi: 0009-0004-6762-9863  
 Selda Ranjbar Salehian: 0000-0002-5223-1332  
 Ahmad Sarostad: 0000-0001-6485-8696  
 Saeideh Ranjbaryan Iri Olya: 0009-0001-9087-2448  
 Maryam Hadizadeh: 0000-0003-1493-0295  
 AmirHossein Khodaei: 0009-0002-0058-415X

## APPENDIX

The appendix tables are related to the extracted TESS primary and secondary times of minima for the V1023 Her and V1397 Her binary systems.

**Table 4.** Extracted times of minima for V1023 Her. All times of minima have been reduced to 2400000. The error value for the minimum times extracted from TESS is 0.0001.

Min.	Epoch	O-C									
58929.7499	-2194.5	0.0051	58944.8956	-2147.5	0.0058	58957.4632	-2108.5	0.0063	58969.7077	-2070.5	0.0059
58929.9136	-2194.0	0.0077	58945.0574	-2147.0	0.0065	58957.6242	-2108.0	0.0062	58969.8693	-2070.0	0.0064
58930.0726	-2193.5	0.0056	58945.2181	-2146.5	0.0061	58957.7855	-2107.5	0.0063	58970.0301	-2069.5	0.0060
58930.2357	-2193.0	0.0076	58945.3803	-2146.0	0.0072	58957.9463	-2107.0	0.0061	58970.1919	-2069.0	0.0068
58930.3944	-2192.5	0.0051	58945.5398	-2145.5	0.0055	58958.1071	-2106.5	0.0057	58970.3522	-2068.5	0.0060
58930.5577	-2192.0	0.0073	58945.7020	-2145.0	0.0066	58958.2691	-2106.0	0.0066	58970.5138	-2068.0	0.0064
58930.7173	-2191.5	0.0059	58945.8625	-2144.5	0.0060	58958.4296	-2105.5	0.0059	58970.6746	-2067.5	0.0061
58930.8803	-2191.0	0.0077	58946.0243	-2144.0	0.0067	58958.5910	-2105.0	0.0063	58970.9964	-2066.5	0.0056
58931.0397	-2190.5	0.0060	58946.1842	-2143.5	0.0055	58958.7520	-2104.5	0.0061	58971.1584	-2066.0	0.0065
58931.2020	-2190.0	0.0071	58946.3465	-2143.0	0.0067	58958.9131	-2104.0	0.0061	58971.3188	-2065.5	0.0059
58931.3629	-2189.5	0.0069	58946.5070	-2142.5	0.0060	58959.0744	-2103.5	0.0063	58971.4799	-2065.0	0.0058
58931.5246	-2189.0	0.0075	58946.6690	-2142.0	0.0070	58959.2352	-2103.0	0.0060	58971.6417	-2064.5	0.0065
58931.6840	-2188.5	0.0058	58946.8284	-2141.5	0.0052	58959.3966	-2102.5	0.0063	58971.8027	-2064.0	0.0064
58931.8467	-2188.0	0.0074	58946.9914	-2141.0	0.0071	58959.5575	-2102.0	0.0061	58971.9639	-2063.5	0.0064
58932.0064	-2187.5	0.0060	58947.1505	-2140.5	0.0051	58959.7187	-2101.5	0.0062	58972.1251	-2063.0	0.0065
58932.1692	-2187.0	0.0077	58947.3135	-2140.0	0.0069	58959.8796	-2101.0	0.0059	58972.2863	-2062.5	0.0066
58932.3284	-2186.5	0.0057	58947.4728	-2139.5	0.0052	58960.0405	-2100.5	0.0057	58972.4472	-2062.0	0.0064
58932.4914	-2186.0	0.0076	58947.6359	-2139.0	0.0072	58960.2026	-2100.0	0.0067	58972.6080	-2061.5	0.0060
58932.6508	-2185.5	0.0059	58947.7953	-2138.5	0.0054	58960.3632	-2099.5	0.0061	58972.7694	-2061.0	0.0064
58932.8136	-2185.0	0.0076	58947.9579	-2138.0	0.0069	58960.5246	-2099.0	0.0065	58972.9305	-2060.5	0.0063
58932.9731	-2184.5	0.0059	58948.1174	-2137.5	0.0053	58960.6851	-2098.5	0.0059	58973.0918	-2060.0	0.0066
58933.1355	-2184.0	0.0073	58948.2802	-2137.0	0.0070	58960.8468	-2098.0	0.0064	58973.2527	-2059.5	0.0064
58933.2953	-2183.5	0.0059	58948.4397	-2136.5	0.0053	58961.0071	-2097.5	0.0056	58973.4140	-2059.0	0.0065
58933.4581	-2183.0	0.0076	58948.6028	-2136.0	0.0073	58961.1688	-2097.0	0.0062	58973.5749	-2058.5	0.0063
58933.6171	-2182.5	0.0056	58948.7622	-2135.5	0.0056	58961.3296	-2096.5	0.0059	58973.7366	-2058.0	0.0069
58933.7806	-2182.0	0.0079	58948.9246	-2135.0	0.0068	58961.4913	-2096.0	0.0064	58973.8969	-2057.5	0.0061
58933.9397	-2181.5	0.0058	58949.0847	-2134.5	0.0059	58961.6521	-2095.5	0.0061	58974.0583	-2057.0	0.0064
58934.1028	-2181.0	0.0079	58949.2469	-2134.0	0.0070	58961.8135	-2095.0	0.0064	58974.2188	-2056.5	0.0057
58934.2621	-2180.5	0.0060	58949.4067	-2133.5	0.0056	58961.9739	-2094.5	0.0057	58974.3809	-2056.0	0.0067
58934.4243	-2180.0	0.0072	58949.5686	-2133.0	0.0064	58962.1355	-2094.0	0.0062	58974.5411	-2055.5	0.0058
58934.5845	-2179.5	0.0063	58949.7295	-2132.5	0.0062	58962.2963	-2093.5	0.0059	58974.7030	-2055.0	0.0066
58934.7467	-2179.0	0.0073	58949.8912	-2132.0	0.0068	58962.4576	-2093.0	0.0060	58974.8634	-2054.5	0.0059
58934.9068	-2178.5	0.0062	58950.0514	-2131.5	0.0058	58962.6184	-2092.5	0.0057	58975.0253	-2054.0	0.0066
58935.0688	-2178.0	0.0072	58950.2133	-2131.0	0.0067	58962.7799	-2092.0	0.0061	58975.1854	-2053.5	0.0056
58935.5514	-2176.5	0.0064	58950.3735	-2130.5	0.0057	58962.9409	-2091.5	0.0060	58975.3476	-2053.0	0.0067
58935.7133	-2176.0	0.0072	58950.5350	-2130.0	0.0061	58963.1025	-2091.0	0.0064	58975.5086	-2052.5	0.0066
58935.8730	-2175.5	0.0057	58950.6962	-2129.5	0.0062	58963.2625	-2090.5	0.0054	58975.6705	-2052.0	0.0073
58936.0356	-2175.0	0.0073	58950.8576	-2129.0	0.0065	58963.4244	-2090.0	0.0062	58975.8304	-2051.5	0.0061
58936.1955	-2174.5	0.0060	58951.0177	-2128.5	0.0055	58963.5852	-2089.5	0.0058	58975.9921	-2051.0	0.0068
58936.3580	-2174.0	0.0074	58951.1797	-2128.0	0.0064	58963.7469	-2089.0	0.0064	58976.1527	-2050.5	0.0062
58936.5177	-2173.5	0.0060	58951.3405	-2127.5	0.0060	58963.9077	-2088.5	0.0061	58976.3141	-2050.0	0.0065
58936.6801	-2173.0	0.0073	58951.5024	-2127.0	0.0068	58964.0680	-2088.0	0.0053	58976.4748	-2049.5	0.0061
58936.8399	-2172.5	0.0059	58951.6625	-2126.5	0.0058	58964.2296	-2087.5	0.0057	58976.6366	-2049.0	0.0068
58937.0022	-2172.0	0.0072	58951.8243	-2126.0	0.0065	58964.3912	-2087.0	0.0062	58976.7968	-2048.5	0.0058
58937.1623	-2171.5	0.0061	58951.9850	-2125.5	0.0060	58964.5518	-2086.5	0.0057	58976.9591	-2048.0	0.0070
58937.3245	-2171.0	0.0072	58952.1469	-2125.0	0.0068	58964.7131	-2086.0	0.0059	58977.1190	-2047.5	0.0058
58937.4839	-2170.5	0.0055	58952.3068	-2124.5	0.0056	58964.8747	-2085.5	0.0064	58977.2812	-2047.0	0.0069
58937.6464	-2170.0	0.0068	58952.4686	-2124.0	0.0064	58965.0355	-2085.0	0.0061	58977.4409	-2046.5	0.0055
58937.8071	-2169.5	0.0064	58952.6293	-2123.5	0.0059	58965.1964	-2084.5	0.0058	58977.6032	-2046.0	0.0067
58937.9691	-2169.0	0.0073	58952.7910	-2123.0	0.0065	58965.3576	-2084.0	0.0059	58977.7636	-2045.5	0.0060
58938.1287	-2168.5	0.0058	58952.9514	-2122.5	0.0058	58965.5183	-2083.5	0.0055	58977.9258	-2045.0	0.0070
58938.2913	-2168.0	0.0073	58953.1130	-2122.0	0.0062	58965.6803	-2083.0	0.0064	58978.0856	-2044.5	0.0057
58938.4510	-2167.5	0.0059	58953.2739	-2121.5	0.0060	58965.8406	-2082.5	0.0056	58978.2479	-2044.0	0.0069
58938.6136	-2167.0	0.0074	58953.4355	-2121.0	0.0065	58966.0030	-2082.0	0.0069	58978.4074	-2043.5	0.0053
58938.7734	-2166.5	0.0061	58953.5960	-2120.5	0.0059	58966.1624	-2081.5	0.0052	58978.5707	-2043.0	0.0074
58938.9355	-2166.0	0.0071	58953.7574	-2120.0	0.0062	58966.3249	-2081.0	0.0065	58978.7300	-2042.5	0.0057
58939.0951	-2165.5	0.0055	58953.9185	-2119.5	0.0062	58966.4848	-2080.5	0.0053	58978.8920	-2042.0	0.0065
58939.2576	-2165.0	0.0069	58954.0797	-2119.0	0.0062	58966.6475	-2080.0	0.0069	58979.0523	-2041.5	0.0057
58939.4173	-2164.5	0.0055	58954.2405	-2118.5	0.0059	58966.8076	-2079.5	0.0059	58979.2144	-2041.0	0.0067
58939.5804	-2164.0	0.0074	58954.4023	-2118.0	0.0067	58966.9693	-2079.0	0.0065	58979.3746	-2040.5	0.0058
58939.7398	-2163.5	0.0058	58954.5629	-2117.5	0.0060	58967.1291	-2078.5	0.0051	58979.5367	-2040.0	0.0068
58939.9025	-2163.0	0.0074	58954.7245	-2117.0	0.0066	58967.2916	-2078.0	0.0066	58979.6969	-2039.5	0.0059
58940.0617	-2162.5	0.0055	58955.8522	-2113.5	0.0065	58967.4527	-2077.5	0.0065	58979.8588	-2039.0	0.0066
58940.2246	-2162.0	0.0072	58956.0127	-2113.0	0.0059	58967.6133	-2077.0	0.0060	58980.0184	-2038.5	0.0051
58940.3841	-2161.5	0.0056	58956.1748	-2112.5	0.0068	58967.7740	-2076.5	0.0056	58980.1816	-2038.0	0.0072
58940.5466	-2161.0	0.0070	58956.3355	-2112.0	0.0064	58967.9357	-2076.0	0.0062	58980.3409	-2037.5	0.0053
58940.7069	-2160.5	0.0062	58956.4970	-2111.5	0.0068	58968.0972	-2075.5	0.0065	58980.5035	-2037.0	0.0068
58944.4140	-2149.0	0.0075	58956.6578	-2111.0	0.0065	58968.2581	-2075.0	0.0064	58980.6635	-2036.5	0.0057
58944.5733	-2148.5	0.0058	58956.8197	-2110.5	0.0072	58969.3854	-2071.5	0.0058	58980.8256	-2036.0	0.0068
58944.7352	-2148.0	0.0066	58957.3020	-2109.0	0.0062	58969.5470	-2071.0	0.0063	58980.9855	-2035.5	0.0055

**Table 5.** Continued for V1023 Her.

Min.	Epoch	O-C	Min.	Epoch	O-C	Min.	Epoch	O-C	Min.	Epoch	O-C
58981.1479	-2035.0	0.0068	59677.3351	125.5	0.0072	59691.3486	169.0	0.0035	59706.1715	215.0	0.0037
58981.3076	-2034.5	0.0054	59677.4930	126.0	0.0040	59693.1246	174.5	0.0072	59706.3371	215.5	0.0081
58981.4704	-2034.0	0.0071	59677.6573	126.5	0.0072	59693.2824	175.0	0.0039	59706.4937	216.0	0.0036
58981.6294	-2033.5	0.0049	59677.8156	127.0	0.0044	59693.4468	175.5	0.0072	59706.6590	216.5	0.0078
58981.7926	-2033.0	0.0071	59677.9795	127.5	0.0071	59693.6049	176.0	0.0042	59706.8159	217.0	0.0036
58981.9516	-2032.5	0.0049	59678.1377	128.0	0.0042	59696.9916	186.5	0.0075	59706.9812	217.5	0.0078
58982.1145	-2032.0	0.0066	59678.3021	128.5	0.0075	59697.1495	187.0	0.0042	59710.0380	227.0	0.0033
59665.4117	88.5	0.0065	59683.4580	144.5	0.0076	59697.3137	187.5	0.0073	59710.2042	227.5	0.0084
59665.5696	89.0	0.0032	59683.6159	145.0	0.0045	59697.4712	188.0	0.0037	59710.3601	228.0	0.0032
59669.6010	101.5	0.0067	59683.7794	145.5	0.0068	59697.6361	188.5	0.0075	59710.5258	228.5	0.0078
59669.7583	102.0	0.0029	59683.9376	146.0	0.0039	59697.7938	189.0	0.0040	59710.6819	229.0	0.0028
59669.9238	102.5	0.0073	59684.1022	146.5	0.0074	59697.9583	189.5	0.0074	59710.8486	229.5	0.0084
59670.0807	103.0	0.0031	59684.2594	147.0	0.0035	59698.1158	190.0	0.0038	59711.0044	230.0	0.0031
59670.2454	103.5	0.0066	59684.4243	147.5	0.0073	59698.2804	190.5	0.0073	59711.1707	230.5	0.0082
59670.4036	104.0	0.0037	59684.5821	148.0	0.0039	59698.4379	191.0	0.0036	59711.3272	231.0	0.0036
59670.5681	104.5	0.0071	59684.7464	148.5	0.0072	59698.6028	191.5	0.0075	59711.4928	231.5	0.0081
59670.7251	105.0	0.0030	59684.9042	149.0	0.0038	59698.7596	192.0	0.0032	59711.6489	232.0	0.0030
59670.8896	105.5	0.0064	59685.0690	149.5	0.0075	59698.9248	192.5	0.0073	59711.8150	232.5	0.0080
59671.0478	106.0	0.0035	59685.2265	150.0	0.0038	59699.0824	193.0	0.0037	59711.9713	233.0	0.0032
59671.2124	106.5	0.0070	59685.3906	150.5	0.0068	59699.2473	193.5	0.0074	59712.1376	233.5	0.0084
59671.3700	107.0	0.0034	59685.5490	151.0	0.0041	59699.4044	194.0	0.0035	59712.2934	234.0	0.0031
59671.5338	107.5	0.0061	59685.7132	151.5	0.0072	59699.5693	194.5	0.0073	59712.4592	234.5	0.0078
59671.6922	108.0	0.0034	59685.8713	152.0	0.0042	59699.7266	195.0	0.0034	59712.6159	235.0	0.0034
59671.8567	108.5	0.0068	59686.0356	152.5	0.0074	59699.8913	195.5	0.0070	59712.7815	235.5	0.0078
59672.0144	109.0	0.0034	59686.1934	153.0	0.0041	59700.0490	196.0	0.0036	59712.9380	236.0	0.0032
59672.1789	109.5	0.0068	59686.3574	153.5	0.0070	59700.2139	196.5	0.0073	59713.1040	236.5	0.0081
59672.5010	110.5	0.0066	59686.5158	154.0	0.0042	59700.3709	197.0	0.0033	59713.2601	237.0	0.0031
59672.6591	111.0	0.0036	59686.6797	154.5	0.0070	59700.5357	197.5	0.0070	59713.4259	237.5	0.0077
59672.8232	111.5	0.0066	59686.8378	155.0	0.0040	59700.6932	198.0	0.0033	59713.5826	238.0	0.0033
59672.9812	112.0	0.0035	59687.0021	155.5	0.0072	59700.8586	198.5	0.0076	59713.7479	238.5	0.0075
59673.1458	112.5	0.0069	59687.1601	156.0	0.0041	59701.0159	199.0	0.0038	59713.9046	239.0	0.0031
59673.3034	113.0	0.0035	59687.3245	156.5	0.0074	59701.1807	199.5	0.0075	59714.0703	239.5	0.0078
59673.4683	113.5	0.0072	59687.4824	157.0	0.0041	59701.3376	200.0	0.0033	59714.2265	240.0	0.0028
59673.6257	114.0	0.0035	59687.6464	157.5	0.0070	59701.5027	200.5	0.0073	59714.3929	240.5	0.0081
59673.7901	114.5	0.0068	59687.8048	158.0	0.0043	59701.6601	201.0	0.0035	59714.5490	241.0	0.0031
59673.9480	115.0	0.0035	59687.9689	158.5	0.0072	59701.8249	201.5	0.0072	59714.7150	241.5	0.0079
59674.1125	115.5	0.0069	59688.1271	159.0	0.0043	59701.9823	202.0	0.0035	59714.8710	242.0	0.0028
59674.2701	116.0	0.0034	59688.2904	159.5	0.0065	59702.1471	202.5	0.0071	59715.0370	242.5	0.0077
59674.4348	116.5	0.0070	59688.4492	160.0	0.0043	59702.3049	203.0	0.0039	59715.1932	243.0	0.0028
59674.5924	117.0	0.0035	59688.6128	160.5	0.0067	59702.4697	203.5	0.0075	59715.3593	243.5	0.0078
59674.7568	117.5	0.0068	59688.7714	161.0	0.0042	59702.6272	204.0	0.0040	59715.5157	244.0	0.0031
59674.9148	118.0	0.0037	59688.9354	161.5	0.0070	59702.7913	204.5	0.0070	59715.6816	244.5	0.0078
59675.0791	118.5	0.0068	59689.0938	162.0	0.0043	59702.9494	205.0	0.0039	59715.8381	245.0	0.0032
59675.2373	119.0	0.0039	59689.2573	162.5	0.0067	59703.1141	205.5	0.0075	59716.0038	245.5	0.0078
59675.4017	119.5	0.0072	59689.4155	163.0	0.0038	59703.2713	206.0	0.0035	59716.1600	246.0	0.0029
59675.5594	120.0	0.0037	59689.5799	163.5	0.0071	59703.4364	206.5	0.0075	59716.3260	246.5	0.0078
59675.7233	120.5	0.0065	59689.7380	164.0	0.0041	59703.5936	207.0	0.0037	59716.4823	247.0	0.0030
59675.8823	121.0	0.0045	59689.9020	164.5	0.0069	59703.7583	207.5	0.0072	59716.6481	247.5	0.0077
59676.0458	121.5	0.0069	59690.0601	165.0	0.0040	59703.9156	208.0	0.0034	59716.8048	248.0	0.0032
59676.2043	122.0	0.0042	59690.2236	165.5	0.0063	59704.0808	208.5	0.0075	59716.9704	248.5	0.0077
59676.3681	122.5	0.0069	59690.3825	166.0	0.0041	59704.2380	209.0	0.0035	59717.1271	249.0	0.0032
59676.5262	123.0	0.0039	59690.5464	166.5	0.0069	59704.4030	209.5	0.0074	59717.2929	249.5	0.0080
59676.6901	123.5	0.0067	59690.7044	167.0	0.0038	59704.5603	210.0	0.0036	59717.4491	250.0	0.0031
59676.8488	124.0	0.0043	59690.8688	167.5	0.0071	59705.7282	213.5	0.0437			
59677.0126	124.5	0.0069	59691.0268	168.0	0.0039	59705.8492	214.0	0.0036			
59677.1714	125.0	0.0046	59691.1911	168.5	0.0071	59706.0149	214.5	0.0081			

**Table 6.** Available times of minima for V1397 Her. All times of minima have been reduced to 2400000. The error value for the minimum times extracted from TESS is 0.0001.

Min.	Epoch	O-C									
58983.7128	13282	0.0439	58993.2124	13306.5	0.0438	59004.0692	13334.5	0.0437	59728.1921	15202	0.0528
58983.9061	13282.5	0.0434	58993.4064	13307	0.0440	59004.2635	13335	0.0441	59728.3864	15202.5	0.0533
58984.1005	13283	0.0439	58993.5999	13307.5	0.0435	59004.4570	13335.5	0.0438	59728.5798	15203	0.0528
58984.2939	13283.5	0.0435	58993.7942	13308	0.0440	59004.6511	13336	0.0440	59728.7736	15203.5	0.0528
58984.4882	13284	0.0439	58993.9877	13308.5	0.0437	59004.8446	13336.5	0.0437	59728.9683	15204	0.0536
58984.6814	13284.5	0.0432	58994.1820	13309	0.0440	59005.0455	13337	0.0507	59729.1614	15204.5	0.0529
58984.8760	13285	0.0439	58994.3758	13309.5	0.0440	59005.2323	13337.5	0.0436	59729.3554	15205	0.0529
58985.0696	13285.5	0.0437	58994.5697	13310	0.0440	59005.4268	13338	0.0443	59729.5488	15205.5	0.0524
58985.2636	13286	0.0438	58994.7634	13310.5	0.0438	59005.6201	13338.5	0.0437	59729.7431	15206	0.0529
58985.4572	13286.5	0.0436	58994.9574	13311	0.0440	59005.8144	13339	0.0441	59729.9369	15206.5	0.0528
58985.6512	13287	0.0437	58995.1510	13311.5	0.0437	59006.0087	13339.5	0.0446	59730.1309	15207	0.0530
58985.8449	13287.5	0.0435	58995.3452	13312	0.0440	59006.2022	13340	0.0442	59731.4879	15210.5	0.0529
58986.0393	13288	0.0440	58995.5389	13312.5	0.0439	59006.3957	13340.5	0.0437	59731.6820	15211	0.0531
58986.2329	13288.5	0.0437	58997.0899	13316.5	0.0439	59006.5900	13341	0.0442	59731.8756	15211.5	0.0528
58986.4269	13289	0.0439	58997.2841	13317	0.0442	59006.7834	13341.5	0.0437	59732.0652	15212	0.0485
58986.6204	13289.5	0.0435	58997.4777	13317.5	0.0439	59006.9777	13342	0.0441	59732.2633	15212.5	0.0528
58986.8143	13290	0.0436	58997.6717	13318	0.0441	59007.1712	13342.5	0.0438	59732.4575	15213	0.0531
58987.0082	13290.5	0.0435	58997.8654	13318.5	0.0439	59007.3655	13343	0.0442	59732.6513	15213.5	0.0530
58987.2023	13291	0.0438	58998.0596	13319	0.0442	59007.5588	13343.5	0.0436	59732.8452	15214	0.0530
58987.3960	13291.5	0.0436	58998.2524	13319.5	0.0431	59007.7532	13344	0.0442	59737.4979	15226	0.0528
58987.5902	13292	0.0439	58998.4472	13320	0.0440	59007.9467	13344.5	0.0438	59737.6917	15226.5	0.0528
58987.7838	13292.5	0.0437	58998.6408	13320.5	0.0438	59008.1410	13345	0.0442	59737.8858	15227	0.0530
58987.9779	13293	0.0438	58998.8351	13321	0.0442	59008.3345	13345.5	0.0439	59738.0794	15227.5	0.0527
58988.1718	13293.5	0.0440	58999.0280	13321.5	0.0433	59008.5286	13346	0.0441	59738.2735	15228	0.0529
58988.3655	13294	0.0437	58999.2227	13322	0.0441	59008.7220	13346.5	0.0436	59738.4671	15228.5	0.0527
58988.5588	13294.5	0.0432	58999.4163	13322.5	0.0438	59008.9165	13347	0.0443	59738.6613	15229	0.0530
58988.7533	13295	0.0438	58999.6106	13323	0.0442	59718.6922	15177.5	0.0527	59738.8547	15229.5	0.0525
58988.9471	13295.5	0.0437	58999.8040	13323.5	0.0438	59718.8861	15178	0.0528	59739.0490	15230	0.0529
58989.1411	13296	0.0438	58999.9982	13324	0.0441	59719.0800	15178.5	0.0527	59739.2434	15230.5	0.0535
58989.3348	13296.5	0.0437	59000.1917	13324.5	0.0437	59719.2739	15179	0.0528	59739.4366	15231	0.0528
58989.5287	13297	0.0437	59000.3860	13325	0.0442	59719.4676	15179.5	0.0526	59739.6304	15231.5	0.0527
58989.7227	13297.5	0.0438	59000.5795	13325.5	0.0438	59719.6617	15180	0.0528	59739.8245	15232	0.0529
58989.9166	13298	0.0438	59000.7738	13326	0.0442	59724.8961	15193.5	0.0527	59740.0085	15232.5	0.0430
58990.1105	13298.5	0.0439	59000.9674	13326.5	0.0439	59725.0901	15194	0.0528	59740.2123	15233	0.0530
58990.3042	13299	0.0437	59001.1616	13327	0.0442	59725.2838	15194.5	0.0527	59740.4060	15233.5	0.0528
58990.4982	13299.5	0.0438	59001.3550	13327.5	0.0438	59725.4778	15195	0.0528	59740.6000	15234	0.0530
58990.6920	13300	0.0438	59001.5491	13328	0.0440	59725.6716	15195.5	0.0527	59740.7938	15234.5	0.0528
58990.8859	13300.5	0.0438	59001.7427	13328.5	0.0437	59725.8655	15196	0.0528	59740.9878	15235	0.0530
58991.0798	13301	0.0438	59001.9370	13329	0.0442	59726.0598	15196.5	0.0531	59741.1815	15235.5	0.0528
58991.2736	13301.5	0.0438	59002.1306	13329.5	0.0439	59726.2532	15197	0.0527	59741.3755	15236	0.0530
58991.4676	13302	0.0438	59002.3246	13330	0.0440	59726.4471	15197.5	0.0528	59741.5693	15236.5	0.0529
58991.6614	13302.5	0.0438	59002.5184	13330.5	0.0439	59726.6410	15198	0.0528	59741.7632	15237	0.0529
58991.8552	13303	0.0437	59002.7123	13331	0.0440	59726.8348	15198.5	0.0526	59741.9570	15237.5	0.0528
58992.0493	13303.5	0.0440	59002.9059	13331.5	0.0437	59727.0289	15199	0.0529	59742.1510	15238	0.0529
58992.2432	13304	0.0440	59003.1003	13332	0.0443	59727.2219	15199.5	0.0520	59742.3441	15238.5	0.0522
58992.4369	13304.5	0.0438	59003.2936	13332.5	0.0436	59727.4164	15200	0.0526	59742.5387	15239	0.0529
58992.6307	13305	0.0437	59003.4879	13333	0.0441	59727.6102	15200.5	0.0526	59742.7326	15239.5	0.0529
58992.8245	13305.5	0.0437	59003.6814	13333.5	0.0437	59727.8047	15201	0.0533	59742.9265	15240	0.0530
58993.0185	13306	0.0438	59003.8756	13334	0.0440	59727.9981	15201.5	0.0528			

## REFERENCES

- Castelli, F., & Kurucz, R. L. 2004, A&A, 419, 725, doi: [10.1051/0004-6361:20040079](https://doi.org/10.1051/0004-6361:20040079)
- Conroy, K. E., Kochoska, A., Hey, D., et al. 2020, ApJS, 250, 34, doi: [10.3847/1538-4365/abb4e2](https://doi.org/10.3847/1538-4365/abb4e2)
- Cox, A. N. 2000, Allen's astrophysical quantities (AN Cox ed)
- Diethelm, R. 2009, Information Bulletin on Variable Stars, 5894, 1
- . 2011, Information Bulletin on Variable Stars, 5992, 1
- . 2012, Information Bulletin on Variable Stars, 6029, 1
- Drake, A. J., Djorgovski, S. G., García-Álvarez, D., et al. 2014, ApJ, 790, 157, doi: [10.1088/0004-637X/790/2/157](https://doi.org/10.1088/0004-637X/790/2/157)
- Eker, Z., Demircan, O., Bilir, S., & Karataş, Y. 2006, MNRAS, 373, 1483, doi: [10.1111/j.1365-2966.2006.11073.x](https://doi.org/10.1111/j.1365-2966.2006.11073.x)
- Eker, Z., Bakış, V., Bilir, S., et al. 2018, MNRAS, 479, 5491, doi: [10.1093/mnras/sty1834](https://doi.org/10.1093/mnras/sty1834)
- Flower, P. J. 1996, ApJ, 469, 355, doi: [10.1086/177785](https://doi.org/10.1086/177785)
- Harmanec, P. 1988, Bulletin of the Astronomical Institutes of Czechoslovakia, 39, 329
- Hubscher, J. 2016, Information Bulletin on Variable Stars, 6157, 1
- Hubscher, J., & Lehmann, P. B. 2015, Information Bulletin on Variable Stars, 6149, 1
- Kazuo, N. 2020, VSOLJ Var. Star Bull, 67
- Kjurkchieva, D. P., Popov, V. A., & Petrov, N. I. 2019, AJ, 158, 186, doi: [10.3847/1538-3881/ab4203](https://doi.org/10.3847/1538-3881/ab4203)
- Kouzuma, S. 2018, PASJ, 70, 90, doi: [10.1093/pasj/psy086](https://doi.org/10.1093/pasj/psy086)
- Kovaleva, D. A. 2002, Astronomy Reports, 46, 233, doi: [10.1134/1.1463101](https://doi.org/10.1134/1.1463101)
- Latković, O., Čeki, A., & Lazarević, S. 2021, ApJS, 254, 10, doi: [10.3847/1538-4365/abeb23](https://doi.org/10.3847/1538-4365/abeb23)
- Li, K., Xia, Q.-Q., Kim, C.-H., et al. 2021, AJ, 162, 13, doi: [10.3847/1538-3881/abfc53](https://doi.org/10.3847/1538-3881/abfc53)
- Lucy, L. B. 1967, ZA, 65, 89
- . 1968, ApJ, 151, 1123, doi: [10.1086/149510](https://doi.org/10.1086/149510)
- Malkov, O. Y. 2007, MNRAS, 382, 1073, doi: [10.1111/j.1365-2966.2007.12086.x](https://doi.org/10.1111/j.1365-2966.2007.12086.x)
- Nelson, R. H. 2015, Information Bulletin on Variable Stars, 6131, 1
- . 2016, Information Bulletin on Variable Stars, 6164, 1
- Nelson, R. H., & Alton, K. B. 2022, Open European Journal on Variable Stars, 234, 1, doi: [10.5817/OEJV2022-0234](https://doi.org/10.5817/OEJV2022-0234)
- O'Connell, D. J. K. 1951, MNRAS, 111, 642, doi: [10.1093/mnras/111.6.642](https://doi.org/10.1093/mnras/111.6.642)
- Paczyński, B. 1967, AcA, 17, 1
- . 1971, ARA&A, 9, 183, doi: [10.1146/annurev.aa.09.090171.001151](https://doi.org/10.1146/annurev.aa.09.090171.001151)
- Pagel, L. 2021, BAV Journal, 52, 1
- . 2022, BAV Journal, 60, 1
- Pogson, N. 1856, MNRAS, 17, 12, doi: [10.1093/mnras/17.1.12](https://doi.org/10.1093/mnras/17.1.12)
- Poro, A., Tanriver, M., Michel, R., & Paki, E. 2024, PASP, 136, 024201, doi: [10.1088/1538-3873/ad1ed3](https://doi.org/10.1088/1538-3873/ad1ed3)
- Poro, A., Hedayatjoo, M., Nastaran, M., et al. 2024, New Astronomy, 110, 102227, doi: <https://doi.org/10.1016/j.newast.2024.102227>
- Poro, A., Paki, E., Alizadehsabegh, A., et al. 2024, Research in Astronomy and Astrophysics, 24, 015002, doi: [10.1088/1674-4527/ad0866](https://doi.org/10.1088/1674-4527/ad0866)
- Prša, A., & Zwitter, T. 2005, ApJ, 628, 426, doi: [10.1086/430591](https://doi.org/10.1086/430591)
- Prša, A., Conroy, K. E., Horvat, M., et al. 2016, ApJS, 227, 29, doi: [10.3847/1538-4365/227/2/29](https://doi.org/10.3847/1538-4365/227/2/29)
- Qian, S. 2003, MNRAS, 342, 1260, doi: [10.1046/j.1365-8711.2003.06627.x](https://doi.org/10.1046/j.1365-8711.2003.06627.x)
- Ruciński, S. M. 1969, AcA, 19, 245
- Salvatier, J., Wieckiā, T. V., & Fonnesbeck, C. 2016, Astrophysics Source Code Library, record ascl:1610.016
- Spada, F., Demarque, P., Kim, Y. C., & Sills, A. 2013, ApJ, 776, 87, doi: [10.1088/0004-637X/776/2/87](https://doi.org/10.1088/0004-637X/776/2/87)
- Terrell, D., Gross, J., & Cooney, W. R. 2012, AJ, 143, 99, doi: [10.1088/0004-6256/143/4/99](https://doi.org/10.1088/0004-6256/143/4/99)
- Torres, G. 2010, AJ, 140, 1158, doi: [10.1088/0004-6256/140/5/1158](https://doi.org/10.1088/0004-6256/140/5/1158)
- Yakut, K., & Eggleton, P. P. 2005, ApJ, 629, 1055, doi: [10.1086/431300](https://doi.org/10.1086/431300)